

RSC Advances



This is an *Accepted Manuscript*, which has been through the Royal Society of Chemistry peer review process and has been accepted for publication.

Accepted Manuscripts are published online shortly after acceptance, before technical editing, formatting and proof reading. Using this free service, authors can make their results available to the community, in citable form, before we publish the edited article. This *Accepted Manuscript* will be replaced by the edited, formatted and paginated article as soon as this is available.

You can find more information about *Accepted Manuscripts* in the [Information for Authors](#).

Please note that technical editing may introduce minor changes to the text and/or graphics, which may alter content. The journal's standard [Terms & Conditions](#) and the [Ethical guidelines](#) still apply. In no event shall the Royal Society of Chemistry be held responsible for any errors or omissions in this *Accepted Manuscript* or any consequences arising from the use of any information it contains.

1 **Organic Hydroperoxide Formation in the Acid-Catalyzed**
2 **Heterogeneous Oxidation of Aliphatic Alcohols with Hydrogen**
3 **Peroxide**

4

5 Qifan Liu, Weigang Wang* , Ze Liu, Tianhe Wang, Lingyan Wu, Maofa Ge*

6 Beijing National Laboratory for Molecular Sciences (BNLMS), State Key Laboratory
7 for Structural Chemistry of Unstable and Stable Species, Institute of Chemistry,
8 Chinese Academy of Sciences, Beijing, 100190, P. R. China

9

10 Corresponding authors:

11 Weigang Wang, phone: +86-10-62558682; email: wangwg@iccas.ac.cn

12 Maofa Ge, phone: +86-10-62554518; email: gemaofa@iccas.ac.cn

13

14

15

16

17

18

19

20

21

22

1 Abstract

2 Organic hydroperoxides (ROOH) are reactive species which play significant roles in
3 atmospheric processes, such as acid precipitation, hydroxyl radicals cycling and
4 secondary organic aerosol formation. Despite their observations in the atmosphere,
5 our understanding of their formation mechanism is still incomplete. In the present
6 work, ROOH formation were found in the acid-catalyzed heterogeneous oxidation of
7 aliphatic alcohols with hydrogen peroxide. The kinetic and mechanism of
8 acid-catalyzed heterogeneous oxidation of three aliphatic alcohols
9 (2-methyl-2-butanol, 3-buten-2-ol and 2-butanol) with hydrogen peroxide were
10 investigated. Based on the experimental results, tertiary or allyl alcohols may
11 contribute to ROOH formation through this route while secondary alcohols may not.
12 The kinetic experiments were conducted in a rotated wetted-wall reactor coupled to a
13 mass spectrometer at room temperature (298K) with 40-70 wt% H₂SO₄ solutions. The
14 reactive uptake coefficients were acquired for the first time. The generation and
15 degradation mechanisms of ROOH in the acidic media were proposed according to
16 the products information. Once formed, ROOH are found to undergo two degradation
17 pathways: the acid-catalyzed rearrangement reaction and organic hydrogen
18 peroxysulfate formation pathway. The newly found acid-catalyzed process may occur
19 under certain conditions and influence particle growth in the atmosphere.

20 Introduction

21 Organic hydroperoxides (ROOH) play significant roles in the atmosphere due to
22 their multiple roles as oxidants and reservoirs of radicals.^{1,2} Moreover, they are

1 considered to be important species of secondary organic aerosol (SOA) and have
2 negative impacts on vegetations.³⁻⁵ A series of ROOH, including methyl
3 hydroperoxide (MHP), hydroxymethyl hydroperoxide (HMHP), and ethyl
4 hydroperoxide (EHP) have been measured in the atmosphere.⁶⁻⁸ Nowadays, it is
5 believed that three reaction pathways may contribute to the formation of ROOH. The
6 bimolecular reaction between organic peroxy radicals (RO_2) and hydroperoxyl
7 radicals (HO_2) is the first route.⁹ The second one is the ozonolysis reaction of
8 alkenes.^{9,10} The third pathway involves reversible addition of hydrogen peroxide
9 (H_2O_2) to aldehydes.¹¹ Here, we propose a new route through oxidation with H_2O_2
10 under acidic conditions that may result in ROOH formation from aliphatic alcohols.

11 Aliphatic alcohols (ROH), an important class of volatile organic compounds, are
12 emitted into the atmosphere by different natural and anthropogenic sources.^{12,13} It
13 could be highly abundant in certain regions, for example, high rates of emission of
14 2-methyl-3-buten-2-ol (MBO) were measured from pine species in western United
15 States.¹⁴⁻¹⁶ It is well recognized that H_2O_2 plays a vital role in both aqueous-phase and
16 gas-phase oxidation.¹⁷ H_2O_2 was observed in cloud water with the concentration
17 ranging from $37.8\mu\text{M}$ to $283.2\mu\text{M}$,¹⁸ and was expected to be present in fine particles
18 at a concentration of 0.1-1mM.¹⁹ On the basis of filter extracts of ambient aerosols
19 and model calculations, Arellanes et al.²⁰ suspected that H_2O_2 concentration in aerosol
20 liquid water might be up to 70mM. Previous field observations and experimental
21 studies²¹⁻²³ have revealed that acid-catalyzed particle-phase reactions of biogenic
22 volatile organic compounds (for example, isoprene and terpenes) or their reactive

1 oxidation products (for example, epoxides) provide a potential source for SOA.
2 Laboratory experiments have also suggested that acid-catalyzed heterogeneous
3 oxidation of isoprene with H_2O_2 makes a contribution to SOA formation.^{24,25} Given
4 the cloud water samples collected from field measurements were often acidic^{26,27} and
5 the estimated pH of liquid aerosol droplets was on the order of -0.8 to 1.18 in
6 northeastern United States,²⁸ heterogeneous reactions of ROH and H_2O_2 in acidic
7 media may take place under certain atmospheric conditions. Previous studies of ROH
8 (for example, methanol, butanol, decanol and MBO) mainly focus on their
9 heterogeneous interactions with sulfuric acid (H_2SO_4) because of their high activities
10 to form organosulfates,²⁹⁻³² these reactions may contribute to aerosol growth. However,
11 the heterogeneous chemistry between ROH and H_2O_2 in acidic media remains largely
12 uncertain. To the best of our knowledge, little attention is paid on the heterogeneous
13 oxidation of ROH with H_2O_2 in the presence of H_2SO_4 , especially a systematic study
14 of heterogeneous interactions between different structures of ROH and H_2O_2 in acidic
15 media is still lacking. Hence, the acid-catalyzed heterogeneous reactions of three
16 different structures of ROH (2-methyl-2-butanol, 3-buten-2-ol and 2-butanol),
17 representing tertiary, allyl and secondary alcohols, respectively, were investigated in
18 this study. The purpose of this research is to gain more knowledge about the uptake
19 kinetics and corresponding chemical mechanisms of diverse structures of ROH into
20 H_2SO_4 - H_2O_2 mixed solution. ROOH, organic peroxides (ROOR) and organosulfates
21 were found to be produced by the heterogeneous process.

22 **Experimental Section**

1 **Uptake Measurements.** The uptake measurements were conducted in a rotated
2 wetted-wall (RWW) flow tube reactor coupled to a signal-photon ionization time of
3 flight mass spectrometer (SPI-TOFMS), similar to our previous study.³³ Briefly, it is a
4 reactor consisted of a Pyrex tube with a glass jacket for thermostatic control. A
5 rotating cylinder (length $L = 30$ cm, inner radius $R = 1.25$ cm, rotating rate $r = 10 \sim 15$
6 rpm) was put into the Pyrex tube, holding small volume of solutions (about 3.5 mL) to
7 form liquid film (about 0.15 mm thickness) evenly on the inner wall. A glass stirring
8 bar was placed on the bottom of the cylinder to ensure that the solution could be
9 mixed and spread sufficiently. To avoid the change of solution composition during
10 one experimental period of time, a mixture of helium (He) and water vapor in
11 equilibrium with the solution was used as carrier gas. Reactant gas was introduced
12 into the reactor at a small flow rate (ten percent of the carrier gas) through a movable
13 glass injector ($D=6$ mm) which was centered in the rotating cylinder. This glass
14 injector allowed for the variation of the contact time between the solution and reactant
15 gas. Typically, the total pressure was in the range of 5.9 to 24.0 Torr and the reactant
16 concentration in the reactor was on the order of 4.8×10^{14} to 1.9×10^{15} molecules cm^{-3} .
17 All of the experiments were carried out at the room temperature (298 K). The
18 Reynolds number calculated was smaller than 2000 under our experimental condition.
19 In this situation, the measurements were operated under the approximate laminar flow
20 condition. Details of SPI-TOFMS are described in the Supplemental Information.

21 **Reactive Uptake Coefficient (γ).** As an uptake experiment just began, the movable
22 injector was placed at the zero position and the solution was unexposed. In this

1 situation, the unperturbed mass signal of reactant gas can be recorded as baseline S_0 .
 2 Then the injector was pulled upstream to expose the solution to the reactant gas and
 3 the signal dropped down simultaneously. Reactive uptake was indicated by a constant
 4 offset between the original signal S_0 and the reactive uptake signal with time, S . The
 5 observed first-order rate constant for removal of the reactant gas from gas-phase, k_{obs}
 6 (s^{-1}) can be calculated from equation 1:

$$7 \quad \ln\left(\frac{S}{S_0}\right) = -k_{obs} \frac{L}{v_{ave}} \quad (1)$$

8 where v_{ave} ($cm\ s^{-1}$) is the average gas flow velocity of the reactant gas, and L (cm) is
 9 the contact distance of the solution and reactant gas. k_{obs} can be determined more
 10 accurately by placing the injector at various positions in the reactor to change the
 11 contact distance. Figure S1a depicts the loss of 2-butanol signal as a function of
 12 injector position. The rate constant for removal of the reactant gas, $k_{gas-liquid}$ (s^{-1}), can
 13 be determined by correcting k_{obs} for diffusion:^{34,35}

$$14 \quad \frac{1}{k_{gas-liquid}} = \frac{1}{k_{obs}} - \frac{1}{k_{diff}} \left(k_{diff} = \frac{3.66D_i}{r^2} \right) \quad (2)$$

15 Where D_i ($cm^2\ s^{-1}$) is the diffusion coefficient which can be calculated from the
 16 Huller-Schettler-Gidding method,³⁶ r (cm) is the inner radius of the rotating cylinder,
 17 and k_{diff} is the diffusion-limited rate (s^{-1}). Finally, the γ can be acquired from equation
 18 3:

$$19 \quad \gamma = \frac{4k_{gas-liquid}V}{\omega A} \quad (3)$$

20 where V (cm^3) is the volume of the reaction zone, A (cm^2) is the geometric area of the
 21 exposed solution, and ω ($m\ s^{-1}$) is the mean molecular speed of reactant alcohol. More

1 calculation details are shown in the Supplemental Information.

2 **Gas-Phase Products Identification.** To further survey the gas-phase products,
3 off-line FTIR spectrometer experiments were performed. The gas-phase species were
4 collected in a U-shape collector located in a liquid nitrogen bath and then analyzed by
5 FTIR spectrometer (Nicolet 6700, Thermo Scientific). The IR spectra provide
6 information about the groups of the products molecules in the spectral range from 650
7 to 4000 cm^{-1} .

8 **Aqueous-Phase Reactions.** Aqueous-phase reactions of ROH (2-butanol,
9 2-methyl-2-butanol, *tert*-butyl alcohol and 3-buten-2-ol) and $\text{H}_2\text{SO}_4\text{-H}_2\text{O}_2$ mixed
10 solution were performed to further study the mechanism. Mixture of 0.1mL ROH and
11 5mL H_2SO_4 (or $\text{H}_2\text{SO}_4\text{-H}_2\text{O}_2$ mixed solution) were shaken thoroughly at 298K for 2h
12 before analysis. Then the mixture was extracted by 2 mL dichloromethane (CH_2Cl_2).
13 To further investigate the formation mechanism of ROOH, 200 mg 2wt% $\text{H}_2^{18}\text{O}_2$ was
14 added into *tert*-amyl sulfate (TAS) solution, which was prepared by the reaction of
15 40mg 2-methyl-2-butanol and 200mg H_2SO_4 (0.2M). Another reaction between 40mg
16 2-methyl-2-butanol and 400mg H_2SO_4 (pH=1)- $\text{H}_2^{18}\text{O}_2$ (1wt%) mixed solution was
17 also conducted. The mixture was extracted by CH_2Cl_2 after 2h reaction. Only the
18 organic-phase after extraction was analyzed by GC-MS and ESI-MS because a large
19 amount of H_2SO_4 remained in the water-phase, hindering the detection of products
20 signals. The pH of the reaction mixture was around 1. This acidity is relevant to the
21 measured range of acidity in atmospheric aerosols.²⁸ As for H_2O_2 , we assume 70mM
22 to be its upper limit in the atmosphere according to previous work.²⁰ 0.1wt% H_2O_2

1 (about 30mM) solutions were used in the uptake measurements and higher
2 concentration (1wt%) of H₂O₂ solutions were used to investigate the mechanism
3 readily. As for the aqueous-phase reactions, considering a certain loss of products in
4 the water-phase, the limit of detection for GC-MS and ESI-MS, high concentration of
5 H₂O₂ (10mM and 300mM) solutions were used during the experiments. GC-MS
6 analysis, ESI-MS analysis and the chemicals used in these experiments are described
7 in the Supplemental Information.

8 **Results and Discussion**

9 **Uptake Behaviors and Kinetics.** Uptake measurements were performed by exposing
10 the gaseous alcohols to a certain length of the H₂SO₄ solution and monitored the
11 MS-signal change meanwhile. Figure 1 depicts the temporal profiles of 2-butanol
12 signals during the uptake measurements. As the H₂SO₄ concentration increased, the
13 uptake behavior of 2-butanol changed from reversible to irreversible. For 50 wt%
14 H₂SO₄ solution, the signal dropped instantly upon exposure and returned to its
15 original level as the solution was saturated. Pushing the injector back to its initial
16 position produced an opposite change in signal, corresponding to the release of
17 2-butanol back to the gas-phase. The similarity in shape and total area of the
18 adsorption and desorption curves implied the occurrence of reversible uptake. For 70
19 wt% H₂SO₄ solution, the uptake displayed a steady-state feature and exhibited no
20 saturation on the time scale of the experiment, indicating that irreversible reactions
21 dominated the uptake process. In a number of experiments, partially irreversible
22 uptake were observed in the variation of the signal (Figure 1b): 2-butanol was found

1 to be taken up and released at a later time, but additionally a constant signal offset
2 was observed. The similar cases were also reported in previous publications.^{30,31}
3 Absorption and desorption likely explain the reversible uptake, the formation of
4 organosulfates and dehydration process could account for the irreversible uptake. For
5 the partially irreversible uptake, a part of gaseous alcohol molecules are physically
6 absorbed while the others could undergo irreversible reactions. The uptake behavior
7 of 3-buten-2-ol was similar with that of 2-butanol. For 2-methyl-2-butanol, reversible
8 uptake was observed for the solution with H₂SO₄ concentration below 40 wt%. The
9 partially irreversible uptake occurred for the 50-60 wt% H₂SO₄ and the uptake on 70
10 wt% H₂SO₄ was totally irreversible. When adding H₂O₂ into H₂SO₄ solution, the
11 steady-state uptake of 2-methyl-2-butanol and 3-buten-2-ol occurred at a lower acidity
12 while the uptake behavior of 2-butanol stayed unchanged.

13 Table 1 summarizes the γ of these three compounds and the corresponding
14 experimental conditions are listed in Table S1. It seems that H₂O₂ plays a role in the
15 enhancement of γ for 2-methyl-2-butanol and 3-buten-2-ol, but has little impact on the
16 uptake of 2-butanol. As for reactive gas uptake, Davidovits et al.³⁷ have suggested that
17 the chemical reactions mainly contribute to the uptake process in many cases.
18 Different chemical mechanisms could be used to explain the diverse uptake behaviors
19 of these compounds. The reactions between ROH and H₂SO₄ at the surface or in the
20 bulk liquid involve two process: dehydration pathway and the formation of
21 organosulfates. When exposing gaseous ROH to H₂SO₄-H₂O₂ mixed solution, a
22 different route that produces ROOH is found except for the reaction of 2-butanol.

1 These reactions are described in detail in the following section. Increasing acidity
2 could result in faster reactions for all three alcohols, thus leading to the enhancement
3 of γ . More concentrated H_2O_2 also accelerates the reaction rates except for that of
4 2-butanol. The γ of these three alcohols under the same experimental conditions (same
5 H_2SO_4 and H_2O_2 concentration) are found to follow the sequence:
6 2-methyl-2-butanol > 3-buten-2-ol > 2-butanol. The generation of carbocation could
7 be a key step either in the dehydration process or the formation of organosulfates and
8 ROOH.³⁸ The stability of carbocations formed during the reactions likely determines
9 the reaction rates which follow the sequence: tertiary > allyl > secondary carbocation.
10 Hence, if the carbocation formation is the central process, it is reasonable that the
11 value of γ for 2-methyl-2-butanol is the biggest among these three alcohols under the
12 same conditions.

13 **Products Identification.** For the uptake of 2-butanol into 70 wt% H_2SO_4 solution
14 (Figure S1b), reactant signals ($m/z=44, 45, 59$ and 74) dropped down as soon as
15 gaseous 2-butanol was exposed to H_2SO_4 solution, meanwhile a new peak at $m/z=56$
16 was detected from the mass spectrum. This peak is ascribed to (E)-2-butene formed
17 through the dehydration of 2-butanol, which is confirmed by the gas-phase products
18 analysis using FTIR spectroscopy (Figure S2b). This result coincides with the
19 Zaitsev's rule (see the Supplemental Information for more details). Aqueous-phase
20 reactions were performed to further survey the products. Figure S3a shows the
21 ESI-MS spectrum (in the negative mode) of extracted organic-phase from
22 aqueous-phase reactions between 2-butanol and H_2SO_4 (pH=1). The peak at $m/z=153$

1 (C₄H₉SO₄⁻) represents the signal of 1-methylpropyl sulfate. Organosulfates were
2 common products formed through this pathway, which were also observed in previous
3 studies.²⁹⁻³² These results indicate that heterogeneous reactions of 2-butanol and
4 H₂SO₄ could result in (E)-2-butene and organosulfates formation.

5 A new peak at m/z=70 appeared in the mass spectrum (Figure 2a) after gaseous
6 2-methyl-2-butanol was exposed to 70 wt% H₂SO₄ solution. An alkene likely
7 accounted for this peak as we found evident resemblance between the gas-phase
8 product IR (Figure S2d) and reference 2-methyl-2-butene IR. Based on the
9 aqueous-phase products analysis, the peak at m/z=167 (C₅H₁₁SO₄⁻) in Figure S3b is
10 due to the generation of organosulfates. These results suggest that organosulfates and
11 alkene are created by the heterogeneous interactions.

12 In contrast to the uptake of 2-methyl-2-butanol on H₂SO₄, obvious changes
13 appeared when adding H₂O₂ into H₂SO₄ solution. As shown in Figure 2b and c,
14 2-methyl-2-butanol signals (m/z=59 and 73) dropped down meanwhile four new
15 peaks at m/z=58, 71, 87 and 104 appeared after the gaseous reactant was exposed to
16 70wt%H₂SO₄-1wt%H₂O₂ mixed solution. Evident changes also appear in the IR
17 spectrum of gas-phase product (Figure S4b), the band at 1740cm⁻¹ is deduced to
18 belong to a C=O stretch. In the light of these results, the peak at m/z=58 detected in
19 the mass spectrum is attributed to the molecule ion of acetone. The peak at m/z = 71
20 (C₅H₁₁⁺) is deduced to be a fragment of *tert*-amyl hydroperoxide (TAHP) according to
21 following experimental evidences. A similar peak was also detected in our previous
22 study on the uptake of MBO into H₂SO₄-H₂O₂ mixed solution:³⁹ in that paper, a new

1 peak at $m/z=69$ was observed through heterogeneous reactions and was ascribed to an
2 online-product which needed to be further identified. The peaks at $m/z=87$ and 104
3 likely stand for TAHP fragment and TAHP molecular ion, respectively. To further
4 investigate this reaction pathway, a series of experiments of aqueous-phase reactions
5 were performed. Figure S5a shows the gas chromatogram of the extracted
6 organic-phase from aqueous-phase reactions of 2-methyl-2-butanol and
7 $H_2SO_4(pH=1)-H_2O_2(300mM)$ mixed solution. Peaks 1-4 in the chromatogram
8 correspond to butane, acetone, solvent dichloromethane and reactant
9 2-methyl-2-butanol, respectively, all of these mass spectra match excellently with
10 those from the MS library. Due to the lack of mass spectra of possible products
11 (TAHP and di-*tert*-amyl peroxide (DTAP)) in the MS library, liquid TAHP and
12 DTAP were injected into GC-MS to obtain the corresponding mass spectra.
13 Additionally, aqueous-phase reactions of *tert*-butyl alcohol and $H_2SO_4-H_2O_2$ mixed
14 solution were also performed in the same experimental conditions because of the
15 similar structure of these two compounds, the products were identified using GC-MS.
16 Therefore, we infer that peak 5 and 6 in Figure S5a belongs to TAHP and DTAP
17 signals respectively for several reasons: (i) Mass spectrum of peak 5 in Figure S5a is
18 nearly the same as that of TAHP, obvious resemblance is also found between the
19 mass spectrum of peak 6 and that of DTAP. (ii) According to the GC-MS results,
20 *tert*-butyl hydroperoxide and di-*tert*-butyl peroxide are found to be produced during
21 the aqueous-phase reactions of *tert*-butyl alcohol and $H_2SO_4-H_2O_2$ mixed solution.
22 Considering the similar structure of 2-methyl-2-butanol and *tert*-butyl alcohol, ROOH

1 maybe also formed from the reaction of 2-methyl-2-butanol and $\text{H}_2\text{SO}_4\text{-H}_2\text{O}_2$ mixed
2 solution. (iii) In the realm of organic chemistry, TAHP and DTAP could be
3 synthesized by the reaction of *tert*-amyl alcohol and $\text{H}_2\text{SO}_4\text{-H}_2\text{O}_2$ mixed solution,
4 which was under very strict control.⁴⁰ (iv) Acetone and butane provide an indirect
5 evidence for the formation of DTAP because they are suggested to be the main
6 pyrolysis products of DTAP at 523K (see Figure S6a for detailed mechanism).⁴⁰
7 Considering the inlet temperature of GC-MS was set at 523K, acetone and butane
8 might be formed through this pathway. TAHP and DTAP were also generated in
9 $\text{H}_2\text{SO}_4(\text{pH}=1)\text{-H}_2\text{O}_2(10\text{mM})$ mixed solution (see Figure S5b).

10 Compared to the aqueous-phase reactions between 2-methyl-2-butanol and
11 H_2SO_4 , a new peak at $m/z=183$ ($\text{C}_5\text{H}_{11}\text{SO}_5^-$) appeared in the ESI-MS spectrum of
12 extracted organic-phase from the reaction between 2-methyl-2-butanol and
13 $\text{H}_2\text{SO}_4\text{-H}_2\text{O}_2$ mixed solution (Figure S3c). This peak was inferred to be related to
14 *tert*-amyl hydrogen peroxysulfate (TAPS), which was produced by the reaction of
15 TAHP and H_2SO_4 . In order to confirm our hypothesis, both the uptake of gaseous
16 TAHP on H_2SO_4 solution and the aqueous-phase reactions between TAHP and H_2SO_4
17 were conducted. The same peak at $m/z=183$ obtained from the ESI-MS (Figure S3d)
18 was also found during the aqueous-phase reactions of TAHP and H_2SO_4 . Figure 3a
19 depicts the mass spectrum of TAHP and five peaks ($m/z=58, 59, 71, 87$ and 104) are
20 observed. These peaks have a good agreement with the peaks shown in Figure 2c.
21 Exposing gaseous THAP to H_2SO_4 (Figure 3b) led to an increment of the signal
22 intensity for the peak at $m/z=58$ while other peaks dropped to a certain extent at the

1 same time. Although the peak at $m/z=58$ is one of fragments of TAHP, we suppose
2 acetone makes a main contribution to peak at $m/z=58$ in Figure 2c for three reasons: (i)
3 The peak at $m/z=58$ in Figure 2c is the strongest fragment, which can hardly caused
4 only by the fragment of TAHP according to the relative peak intensity between the
5 molecular ion peak at $m/z=104$ and fragment peak at $m/z=58$ (shown in Figure 3a). (ii)
6 Figure S4d shows the IR spectrum of products formed in the heterogeneous reaction
7 of TAHP and H_2SO_4 , the band around 1740 cm^{-1} allows a straightforward detection of
8 C=O stretching modes. This result gives a strong support to the formation of carbonyl
9 compounds. (iii) Acetone may be formed through the protolytic
10 cleavage-rearrangement reactions of TAHP in acidic media according to previous
11 work.⁴¹ Based on all these experimental evidences, TAHP, DTAP, TAPS and acetone
12 are considered to be generated by the heterogeneous reactions of 2-methyl-2-butanol
13 and H_2SO_4 - H_2O_2 mixed solution. Detailed reaction mechanism is discussed in the
14 subsequent section.

15 As for the uptake of 3-buten-2-ol in H_2SO_4 solution (Figure 3c), the reactant
16 signals ($m/z=43$, 57 and 72) decreased quickly after gaseous 3-buten-2-ol was
17 exposed to H_2SO_4 , simultaneously a new peak at $m/z = 54$ appeared. Similar to the
18 uptake of former two alcohols, this peak is caused by an alkene because the product
19 IR (Figure S2f) is nearly the same as the reference 1,3-butadiene IR. In the light of
20 ESI-MS result (Figure S3e), the peak at $m/z=151$ ($C_4H_7SO_4^-$) is inferred to be
21 1-methylallyl sulfate signal, just like the reactions of former two alcohols and H_2SO_4 .

1 Figure 3e shows the temporal profiles of all ion peaks during the uptake of
2 3-buten-2-ol into 70wt% H_2SO_4 -1wt% H_2O_2 mixed solution, and Figure 3f is the
3 real-time mass spectrum after exposure. The 3-buten-2-ol signals dropped down as
4 soon as the reaction started and two new peaks at $m/z=44$ and 55 appeared. The peak
5 at $m/z=55$ (C_4H_7^+) is 1 amu larger than the dehydration product 1,3-butadiene. The
6 similar cases also occurred in the uptake experiments of MBO and
7 2-methyl-2-butanol.³⁹ Consequently, we infer methylallyl hydroperoxide (MAHP) is
8 generated by this heterogeneous reaction and the peak at $m/z=55$ is one of its
9 fragments. As shown in Figure S4f, a strong band around 1745 cm^{-1} is observed in
10 gas-phase products, which should be caused by carbonyl compounds. On the basis of
11 these results, the peak at $m/z = 44$ in Figure 3f is inferred to belong to the molecular
12 ion of acetaldehyde. The reaction pathway is discussed in detail in the following
13 section. Due to the lack of standard compound, the information about the mass
14 spectrum of MAHP is limited and the aqueous-phase products were only analyzed by
15 ESI-MS. As mentioned above, organic hydrogen peroxysulfate (ROOSO_3H) is
16 created by the reaction of ROOH and H_2SO_4 . Therefore, if MAHP was formed in the
17 aqueous-phase reactions, ROOSO_3H should be detected by ESI-MS. The peak at
18 $m/z=167$ ($\text{C}_4\text{H}_7\text{SO}_5^-$) (Figure S3f) is deduced to be 1-methylallyl hydrogen
19 peroxysulfate signal. These results reveal that ROOH are also formed through the
20 acid-catalyzed oxidation of 3-buten-2-ol with H_2O_2 .

21 **Reaction Mechanism.** As stated above, TAHP, DTAP, TAPS and acetone are
22 considered to be produced by the heterogeneous reactions of 2-methyl-2-butanol and

1 H₂SO₄-H₂O₂ mixed solution. Combining the results obtained from SPI-TOFMS, FTIR
2 spectrometer, GC-MS, ESI-MS and previous research,⁴⁰ the proposed chemical
3 mechanism for the formation and degradation of TAHP is shown in Figure 4. The
4 initial step involves the addition of a proton to the hydroxyl of 2-methyl-2-butanol
5 followed by the elimination of H₂O and generation of tertiary carbocations. Based on
6 the previous studies, ROOH may be prepared by nucleophilic attack of concentrated
7 H₂O₂ on carbonium ions and the reaction is proposed to follow an S_N1 pathway.^{38,41}
8 Considering HO₂⁻ (caused by heterolysis of H₂O₂) is a strong nucleophile, the possible
9 ROOH formation mechanism is HO₂⁻ attack the carbocations. Thus, HO₂⁻ or hydrogen
10 sulfate ion (HSO₄⁻) could attack carbocations in the following step, giving TAHP and
11 organosulfates, respectively. In the realm of organic chemistry, TAHP was
12 synthesized based on the method introduced by Milas and Surgenor:⁴⁰ adding
13 concentrated H₂O₂ into *tert*-amyl sulfate (TAS) solution (prepared by reaction of
14 2-methyl-2-butanol and H₂SO₄) could lead to the generation of TAHP (main product)
15 and DTAP (byproduct). Under this condition, HO₂⁻ or OH⁻ may attack different
16 positions of TAS, thus producing TAHP. To the best of our knowledge, in previous
17 literature little attention was paid to the question that which route might be the main
18 pathway. To get a better understanding of the chemical mechanism, two experiments
19 are designed: the first one is adding H₂¹⁸O₂ into TAS, the other one is adding
20 2-methyl-2-butanol into mixed H₂SO₄-H₂¹⁸O₂ solution. As shown in Figure 4, if HO₂⁻
21 pathway is the main route, TAHP formed by this way will further react with H₂SO₄,
22 thus a peak at m/z=185 (C₅H₁₁S¹⁶O₄¹⁸O⁻) should be detected by ESI-MS. Conversely,

1 if OH⁻ pathway controls the reaction, a peak at m/z=183 (C₅H₁₁S¹⁶O₅⁻) should be
2 found. Referring to Figure S3g and h, the peak at m/z=167 is attributed to TAS and
3 the peak at m/z=185 represents the ROOSO₃H formed through HO₂⁻ route. Weak
4 peaks at m/z=183 were also detected, this might be due to the OH⁻ pathway or the
5 influence of H₂¹⁸O₂ (contain 10 atom% ¹⁶O). Considering the strong intensity of the
6 peak at m/z=185, we conclude that HO₂⁻ route is the main pathway.

7 Once generated in H₂SO₄ solution, the degradation of TAHP occurs
8 simultaneously. On one hand, cleavage of oxygen to oxygen (O-O) bond in TAHP
9 produces alkoxy radicals (RO), which then react further with H₂SO₄ to produce
10 TAPS or combine with other RO to form DTAP. On the other hand, TAHP undergoes
11 an acid-catalyzed rearrangement which leads to the formation of acetone. Figure 5
12 depicts the rearrangement mechanism. The cleavage of O-O bond of conjugate acid,
13 caused by the protonation at oxygen atom, leads to the formation of a highly energetic
14 oxenium ion. Then the oxenium ion rearranges to the alkylated ketone immediately,
15 which reacts further to produce acetone and ethanol. The relative migratory ability of
16 different groups follows the trend ethyl > methyl during the rearrangement. Although
17 magic acid (not H₂SO₄) was used in the study of rearrangement of ROOH in previous
18 research,⁴¹ we thought this process could also take place in the presence of H₂SO₄
19 because it was reported that *tert*-butyl hydroperoxide underwent a similar
20 rearrangement reaction in H₂SO₄.⁴² Ethanol is a missing product of the rearrangement
21 process in our study for two reasons: (i) Ethanol tends to stay in the aqueous-phase for
22 its great solubility in water and reacts further with H₂SO₄ to form ethyl sulfate, the

1 similar route is also reported in former paper.⁴² (ii) Even though gaseous ethanol is
2 produced, the SPI-TOFMS can hardly detect it because our instrument can only detect
3 species whose ionization energy is below 10.5eV. Fortunately, according to the
4 products analysis of aqueous-phase reactions between TAHP and H₂SO₄, the peak at
5 m/z=125 (C₂H₅SO₄⁻) (Figure S3d) which is ascribed to ethyl sulfate, gives an indirect
6 evidence for the generation of ethanol. Moreover, when extending the formation
7 mechanism of ROOH to our previous work,³⁹ it is logical to infer that
8 1,1-dimethylallyl hydroperoxide is generated by the uptake of MBO into H₂SO₄-H₂O₂
9 mixed solution. If ROOH formed from MBO undergoes the same rearrangement
10 mechanism just as TAHP does, acetone and acetaldehyde should be the products (see
11 Figure S6b for detailed mechanism). Previous results have shown a good agreement
12 with our conjecture. Considering all this, it is reasonable to conclude that TAHP
13 undergoes a rearrangement reaction in H₂SO₄.

14 As for the chemical mechanism during the reaction of 3-buten-2-ol and H₂SO₄
15 -H₂O₂ mixed solution, ROOH is also formed and follows the same rule as
16 2-methyl-2-butanol undergoes (see Figure S6c for detailed information).
17 Experimental evidence is limited to validate the generation of ROOR, nevertheless, it
18 is a possible route for the formation of methylallyl peroxide during the heterogeneous
19 interaction as DTAP is produced under the similar condition. It is very interesting that
20 H₂O₂ changes the chemical mechanism of 2-methyl-2-butanol and 3-buten-2-ol, while
21 it has no obvious effect on 2-butanol, leading to a higher γ for 2-methyl-2-butanol and
22 3-buten-2-ol. The different reactivity may be caused by the stability of carbocations

1 formed during the reactions: more stable carbocations may contribute to the
2 generation of ROOH while the less stable carbocations may not. Our results are
3 consistent with previous findings.⁴³

4 **Conclusion and Atmospheric Implications**

5 In this work, the γ of three different structures of ROH into H₂SO₄-H₂O₂ mixed
6 solution were calculated and the corresponding chemical pathways were deduced
7 according to the products information. For 2-methyl-2-butanol and 3-buten-2-ol,
8 ROOH, ROOR, ROOSO₃H and organosulfates were found to be created by the
9 heterogeneous interactions. The newly found acid-catalyzed pathway may provide a
10 potential route for ROOH formation and influence particle growth.

11 It has been suggested that the majority of the ROOH in the gas-phase are formed
12 via the recombination reaction of HO₂ and RO₂ during the daytime.⁹ Other
13 mechanisms for the formation of ROOH in the absence of light include the ozonolysis
14 reaction of alkenes^{9,10} and aqueous-phase reaction between H₂O₂ and aldehydes.¹¹
15 Here, we introduce another possible pathway for the formation of ROOH during the
16 acid-catalyzed oxidation of ROH (limited to tertiary or allyl alcohols) with H₂O₂.
17 Tertiary and allyl aliphatic alcohols are emitted into the atmosphere by different
18 natural and anthropogenic sources. For example, a series of tertiary and allyl alcohols
19 are emitted to the atmosphere by plant species,¹³ MBO can be highly abundant in pine
20 forests of the western United States,¹⁴⁻¹⁶ 3-methyl-2-buten-1-ol is an ingredient used
21 in fine fragrances with production of 1-10 metric tons per year.⁴⁴ Hence, considering
22 the high concentration of total release of tertiary and allyl alcohols by pine forests,

1 they may contribute to ROOH formation through the acid-catalyzed reactions.
2 However, only short-chain ($C \leq 2$) ROOH (mainly MHP, EHP and HMHP) have been
3 measured in the environment in the past two decades.⁶⁻⁸ According to the review
4 summarized by Reeves and Penkett,⁴⁵ high performance liquid-phase chromatography
5 with post-column enzyme derivatization is a useful method to detect individual
6 ROOH. Horseradish peroxidase (HRP) was used to catalyze the reduction of ROOH
7 in previous field measurements.^{6-8,46,47} It should be pointed out that HRP can only
8 effectively catalyze the reduction of H_2O_2 and short-chain ($C \leq 2$) ROOH because of its
9 specificity for the hydrogen receptor.⁴⁸ Furthermore, many standards of long-chain
10 ROOH (for example, 1,1-dimethylallyl hydroperoxide) are not available. These two
11 factors may inhibit the measurement of ROOH formed through the acid-catalyzed
12 pathway. Based on the experimental evidence (2-methyltetrols was found to be
13 produced by the reaction of isoprene and H_2SO_4 - H_2O_2 mixed solution) and field
14 measurements, Claeys et al. suggested that multiphase acid-catalyzed oxidation of
15 isoprene with H_2O_2 may contribute to SOA formation.²⁴ Similarly, on the basis of the
16 aqueous-phase reaction results shown in the present work, it seems logical to assume
17 that the acid-catalyzed reactions of ROH may also occur under certain conditions and
18 contribute to ROOH formation. Our results imply that this acid-catalyzed route is a
19 potential source for ROOH formation and more research is needed to elucidate the
20 role of this pathway.

21 The heterogeneous reactions may influence particle growth, especially in the
22 upper troposphere where sulfate aerosols are more concentrated. Organosulfates were

1 deduced to be produced during the acid-catalyzed reactions. They were reported to
2 undergo a slow hydrolysis reaction and likely to be stable during the lifetime of most
3 ambient SOA.^{49,50} The uptake of ROH into existing acidic particles could lead to the
4 formation of low-volatility organosulfates, which tend to stay stable in the
5 particle-phase and contribute to the particles growth. In addition, aldehydes and
6 ketones are found to be generated by the acid-catalyzed rearrangement reaction of
7 ROOH. These carbonyl compounds may undergo aldol condensation and
8 polymerization in the acidic media,^{3,51} thus leading to the formation of
9 higher-molecule weight compounds which may also make a contribution to the
10 particle growth for their low volatility.

11 **Acknowledgements**

12 This research was financially supported by the Strategic Priority Research Program(B)
13 of the Chinese Academy of Sciences (XDB05010400) and National Natural Science
14 Foundation of China (Major Program: 21190052 & Contract No. 41173112,
15 21077109,40925016).

16 **References**

- 17 1 J. G. Calvert, A. Lazrus, G. L. Kok, B. G.Heikes, J. G. Walega, J. Lind and C.
18 A.Cantrell, *Nature* 1985, **317**, 27-35.
- 19 2 F. Ravetta, D. J. Jacob, W. H. Brune, B. G. Heikes, B. E. Anderson, D. R. Blake, G.
20 L.Gregory, G. W. Sachse, S. T. Sandholm, R. E. Shetter, H. B. Singh and R. W.
21 Talbot, *J. Geophys. Res.* 2001, **106**, 32709-32716.
- 22 3 M. Hallquist, J. C.Wenger, U. Baltensperger, Y. Rudich, D. Simpson, M. Claeys, J.
23 Dommen, N. M. Donahue, C. George, A. H. Goldstein, J. F. Hamilton, H. Herrmann,
24 T. Hoffmann, Y. Iinuma, M. Jang, M. E. Jenkin, J. L. Jimenez, A. Kiendler-Scharr,

- 1 W. Maenhaut, G. McFiggans, T. F. Mentel, A. Monod, A. S. H. Prevot, J. H. Seinfeld,
2 J. D. Surratt, R. Szmigielski and J. Wildt, *Atmos. Chem. Phys.* 2009, **9**, 5155-5236.
- 3 4 Q. Chen, Y. J. Liu, N. M. Donahue, J. E. Shilling and S. T. Martin, *Environ. Sci.*
4 *Technol.* 2011, **45**, 4763-4770.
- 5 5 C. N. Hewitt, G. L. Kok and R. Fall, *Nature* 1990, **344**, 56-58.
- 6 6 E. Hellpointner and S. Gab, *Nature* 1989, **337**, 631-634.
- 7 7 C. N. Hewitt and G. L. Kok, *J. Atmos. Chem.* 1991, **12**, 181-194.
- 8 8 J. Valverde-Canossa, W. Wieprecht, K. Acker and G. K. Moortgat, *Atmos. Environ.*
9 2005, **39**, 4279-4290.
- 10 9 K. H. Becker, K. J. Brockmann and J. Bechara, *Nature* 1990, **346**, 256-258.
- 11 10 M. H. Lee, B. G. Heikes and D. W. O'Sullivan, *Atmos. Environ.* 2000, **34**,
12 3475-3494.
- 13 11 R. Zhao, A. K. Y. Lee, R. Soong, A. J. Simpson and J. P. D. Abbatt, *Atmos. Chem.*
14 *Phys.* 2013, **13**, 5857-5872.
- 15 12 P. D. Goldan, W. C. Kuster, F. C. Fehsenfeld and S. A. Montzka, *Geophys. Res.*
16 *Lett.* 1993, **20**, 1039-1042.
- 17 13 G. Konig, M. Brunda, H. Puxbaum, C. N. Hewitt, S. C. Duckham, J. Rudolph,
18 *Atmos. Environ.* 1995, **29**, 861-874.
- 19 14 P. Harley, V. Fridd-Stroud, J. Greenberg, A. Guenther and P. Vasconcellos, *J.*
20 *Geophys. Res.* 1998, **103**, 25479-25486.
- 21 15 M. S. Lamanna and A. H. Goldstein, *J. Geophys. Res.* 1999, **104**, 21247-21262.
- 22 16 N. C. Bouvier-Brown, A. H. Goldstein, D. R. Worton, D. M. Matross, J. B. Gilman,
23 W. C. Kuster, D. Welsh-Bon, C. Warneke, J. A. de Gouw, T. M. Cahill and R.
24 Holzinger, *Atmos. Chem. Phys.* 2009, **9**, 2061-2074.
- 25 17 A. V. Jackson, *Crit. Rev. Environ. Sci. Technol.* 1999, **29**, 175-228.
- 26 18 D. J. Straub, T. Lee and J. L. Collett, *J. Geophys. Res.* 2007, **112**, D04307.
- 27 19 A. S. Hasson and S. E. Paulson, *J. Aerosol. Sci.* 2003, **34**, 459-468.
- 28 20 C. Arellanes, S. E. Paulson, P. M. Fine and C. Sioutas, *Environ. Sci. Technol.* 2006,
29 **40**, 4859-4866.

- 1 21 J. D. Surratt, Y. Gomez-Gonzalez, A. W. H. Chan, R. Vermeylen, M. Shahgholi,
2 T. E. Kleindienst, E. O. Edney, J. H. Offenberg, M. Lewandowski, M. Jaoui, W.
3 Maenhaut, M. Claeys, R. C. Flagan and J. H. Seinfeld, *J. Phys. Chem. A* 2008, **112**,
4 8345-8378.
- 5 22 J. D. Surratt, A. W. H. Chan, N. C. Eddingsaas, M. N. Chan, C. L. Loza, A. J.
6 Kwan, S. P. Hersey, R. C. Flagan, P. O. Wennberg and J. H. Seinfeld, *Proc. Natl.*
7 *Acad. Sci. U. S. A.* 2010, **107**, 6640-6645.
- 8 23 L. E. Hatch, J. M. Creamean, A. P. Ault, J. D. Surratt, M. N. Chan, J. H. Seinfeld,
9 E. S. Edgerton, Y. X. Su and K. A. Prather, *Environ. Sci. Technol.* 2011, **45**,
10 5105-5111.
- 11 24 M. Claeys, W. Wang, A. C. Ion, I. Kourtchev, A. Gelencser and W. Maenhaut,
12 *Atmos. Environ.* 2004, **38**, 4093-4098.
- 13 25 O. Boge, Y. Miao, A. Plewka and H. Herrmann, *Atmos. Environ.* 2006, **40**,
14 2501-2509.
- 15 26 J. Guo, Y. Wang, X. H. Shen, Z. Wang, T. Lee, X. F. Wang, P. H. Li, M. H. Sun,
16 J. L. Collett, W. X. Wang and T. Wang, *Atmos. Environ.* 2012, **60**, 467-476.
- 17 27 E. Harris, B. Sinha, D. van Pinxteren, A. Tilgner, K. W. Fomba, J. Schneider, A.
18 Roth, T. Gnauk, B. Fahlbusch, S. Mertes, T. Lee, J. Collett, S. Foley, S. Borrmann, P.
19 Hoppe and H. Herrmann, *Science* 2013, **340**, 727-730.
- 20 28 R. J. Ferek, A. L. Lazrus, P. L. Haagenson and J. W. Winchester, *Environ. Sci.*
21 *Technol.* 1983, **17**, 315-324.
- 22 29 S. M. Kane and M. T. Leu, *J. Phys. Chem. A* 2001, **105**, 1411-1415.
- 23 30 N. P. Levitt, J. Zhao and R. Y. Zhang, *J. Phys. Chem. A* 2006, **110**, 13215-13220.
- 24 31 B. Noziere, D. Voisin, C. A. Longfellow, H. Friedli, B. E. Henry and D. R. Hanson,
25 *J. Phys. Chem. A* 2006, **110**, 2387-2395.
- 26 32 L. L. Van Loon and H. C. Allen, *J. Phys. Chem. A* 2008, **112**, 7873-7880.
- 27 33 T. H. Wang, Z. Liu, W. G. Wang and M. F. Ge, *Atmos. Environ.* 2012, **56**, 58-64.
- 28 34 D. M. Murphy and D. W. Fahey, *Anal. Chem.* 1987, **59**, 2753-2759.
- 29 35 D. R. Hanson, J. B. Burkholder, C. J. Howard and A. R. Ravishankara, *J. Phys.*
30 *Chem.* 1992, **96**, 4979-4985.

- 1 36 E. N. Fuller, P. D. Schettler and J. C. Giddings, *Ind. Eng. Chem. Res.* 1966, **58**,
2 19-27.
- 3 37 P. Davidovits, C. E. Kolb, L. R. Williams, J. T. Jayne and D. R. Worsnop, *Chem.*
4 *Rev.* 2006, **106**, 1323-1354.
- 5 38 A. G. Davies, R. V. Foster and A. M. White, *J. Chem. Soc.* 1953, **MAY**,
6 1541-1547.
- 7 39 Z. Liu, M. F. Ge, W. G. Wang, S. Yin and S. R. Tong, *Phys. Chem. Chem. Phys.*
8 2011, **13**, 2069-2075.
- 9 40 N. A. Milas and D. M. Surgenor, *J. Am. Chem. Soc.* 1946, **68**, 643-644.
- 10 41 G. A. Olah, D. G. Parker, N. Yoneda and F. Pelizza, *J. Am. Chem. Soc.* 1976, **98**,
11 2245-2250.
- 12 42 N. C. Deno, W. E. Billups, K. E. Kramer and R. R. Lastomir, *J. Org. Chem.* **1970**,
13 **35**, (9), 3080-3082.
- 14 43 R. Criegee and H. Dietrich, *Liebigs. Ann. Chem.* 1948, **560**, 135-141.
- 15 44 D. McGinty, L. Jones, C. S. Letizia and A. M. Api, *Food Chem. Toxicol.* 2010, **48**,
16 S64-S69.
- 17 45 C. E. Reeves and S. A. Penkett, *Chem. Rev.* 2003, **103**, 5199-5218.
- 18 46 Y. Ren, A. J. Ding, T. Wang, X. H. Shen, J. Guo, J. M. Zhang, Y. Wang, P. J. Xu,
19 X. F. Wang, J. Gao and J. L. Collett, *Atmos. Environ.* 2009, **43**, 1702-1711.
- 20 47 R. B. Morgan and A. V. Jackson, *J. Geophys. Res.* 2002, **107**, (D19).
- 21 48 G. G. Guilbault. *Handbook of Enzymatic Methods of Analysis*, Marcel Dekker,
22 New York, 1976.
- 23 49 K. S. Hu, A. I. Darer and M. J. Elrod, *Atmos. Chem. Phys.* 2011, **11**, 8307-8320.
- 24 50 A. I. Darer, N. C. Cole-Filipiak, A. E. O'Connor and M. J. Elrod, *Environ. Sci.*
25 *Technol.* 2011, **45**, 1895-1902.
- 26 51 M. S. Jang, N. M. Czoschke, S. Lee and R. M. Kamens, *Science* 2002, **298**,
27 814-817.
- 28
- 29

1 **Table 1.** Summarization of reactive uptake coefficients for three aliphatic alcohols

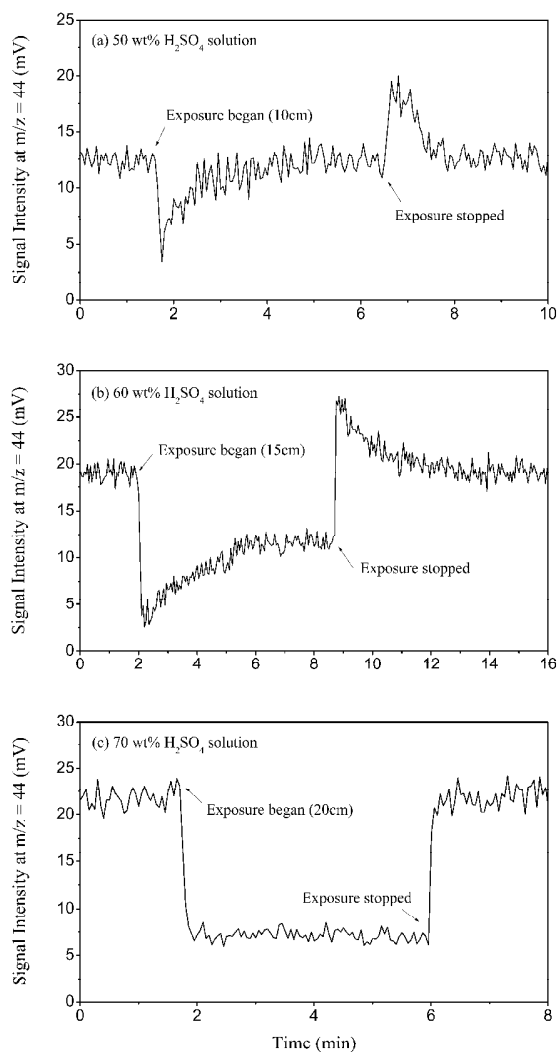
Gas Reactant	H₂SO₄ (wt %)	H₂O₂ (wt %)	γ^\dagger ($\times 10^{-4}$)
2-butanol	60	0	0.98±0.02
	60	1	0.82 ± 0.01
	70	0	1.98± 0.05
	70	1	2.01 ± 0.04
2-methyl-2-butanol	40	0	/
	40	1	0.46 ± 0.02
	50	0	0.27± 0.02
	50	0.1	0.51±0.16
	50	0.5	2.21±0.15
	50	1	5.89±0.12
	60	0	1.99±0.04
	60	0.1	2.93±0.02
	60	0.5	5.65±0.15
	60	1	18.43 ±1.09
	70	0	12.52 ± 0.68
	70	0.1	16.00±0.03
	70	0.5	29.63±0.62
	70	1	66.49 ± 0.64
3-buten-2-ol	50	0	/
	50	1	1.61±0.13
	60	0	1.10±0.07
	60	0.1	1.28±0.04
	60	0.5	1.57±0.04
	60	1	7.60 ± 0.37
	70	0	2.21±0.44
	70	0.1	2.57±0.07
	70	0.5	3.93±0.16
	70	1	17.13 ± 0.32

2

3 / represents no obvious uptake.

4 †Each value is the average of at least three measurements, and the error corresponds

5 to one standard deviation (σ).



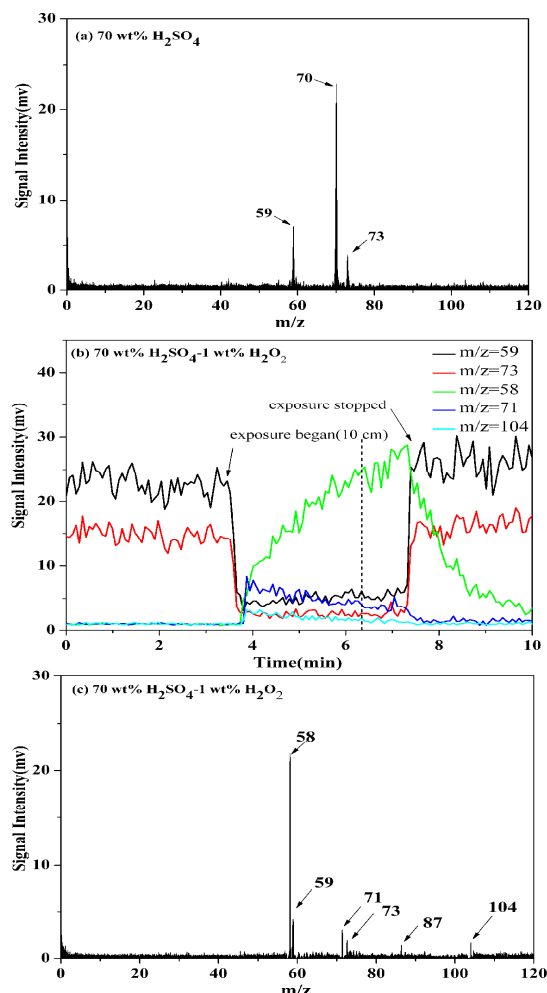
1

2 **Figure 1.** Typical experimental profiles of 2-butanol. (a) reversible uptake into 50
3 wt% H₂SO₄ solution; (b) partially irreversible uptake into 60 wt% H₂SO₄ solution; (c)
4 irreversible uptake into 70 wt% H₂SO₄ solution.

5

6

7



1

2 **Figure 2.** Typical uptake experimental profiles of 2-methyl-2-butanol. (a) The
3 real-time mass spectrum after gas 2-methyl-2-butanol was exposed to 70 wt% H₂SO₄
4 solution; (b) The profiles of monitoring ion peaks in real-time during the uptake of
5 2-methyl-2-butanol into 70wt%H₂SO₄-1 wt% H₂O₂ mixed solution; (c) real-time mass
6 spectrum at the time marked by dash line in (b). The peak at m/z=87 is not shown in
7 (b) because the SPI-TOFMS can only monitor five peaks at one time.

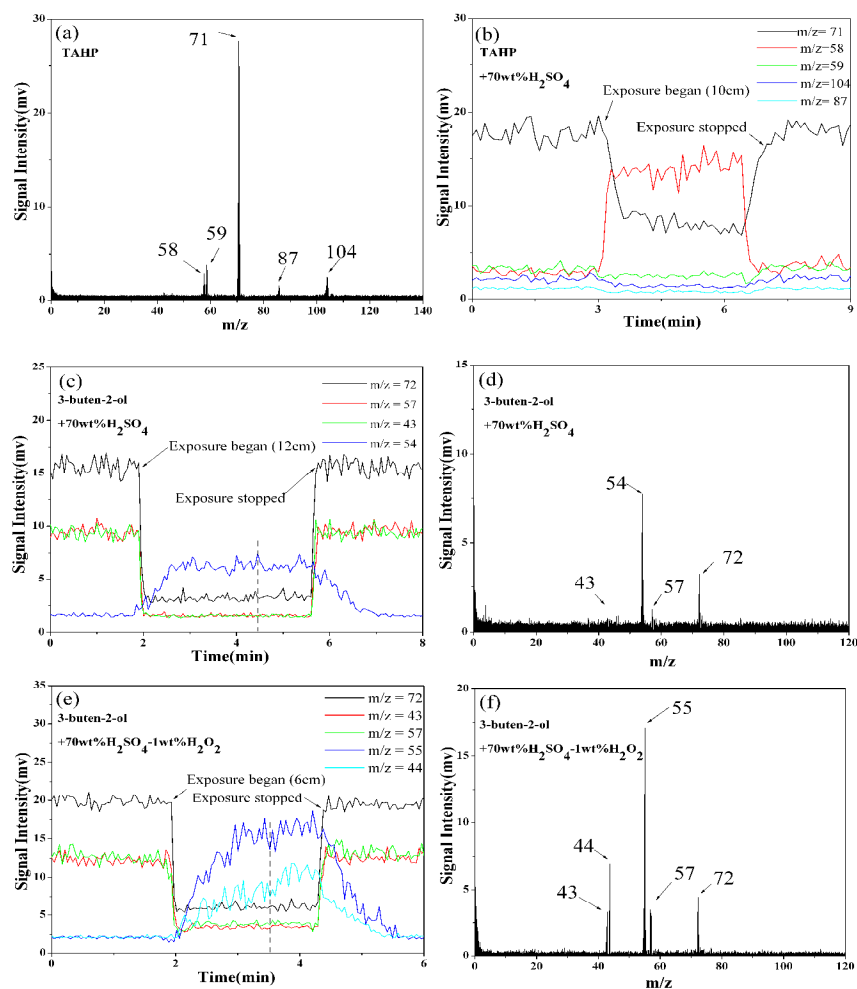
8

9

10

11

12

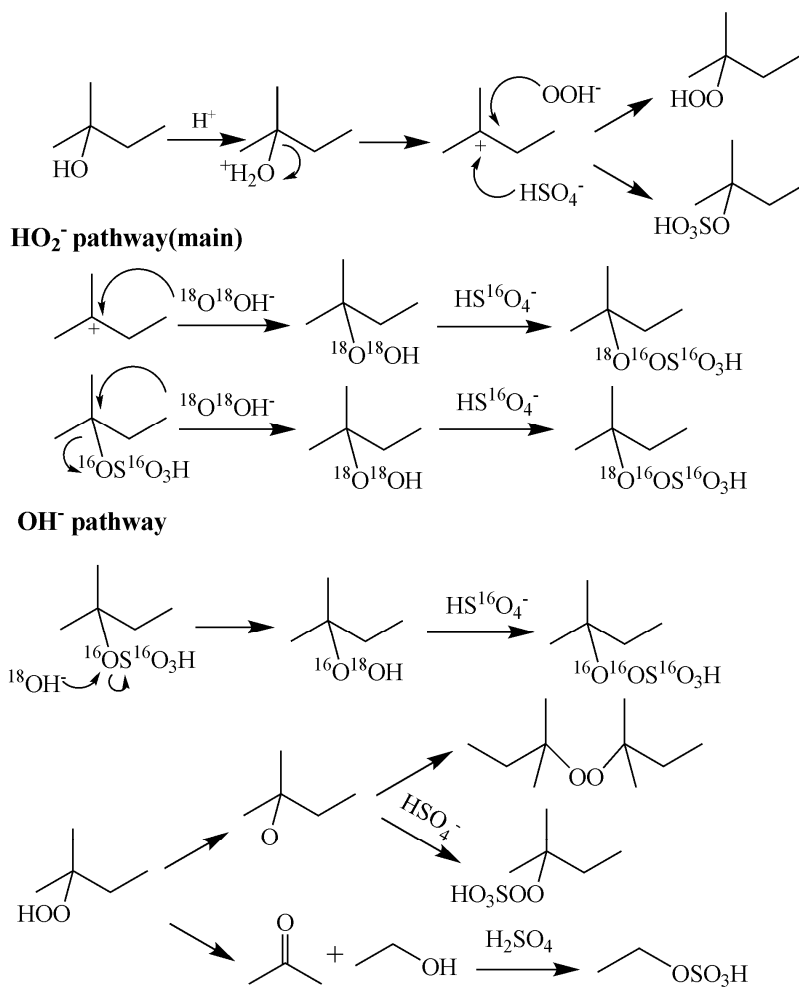


1

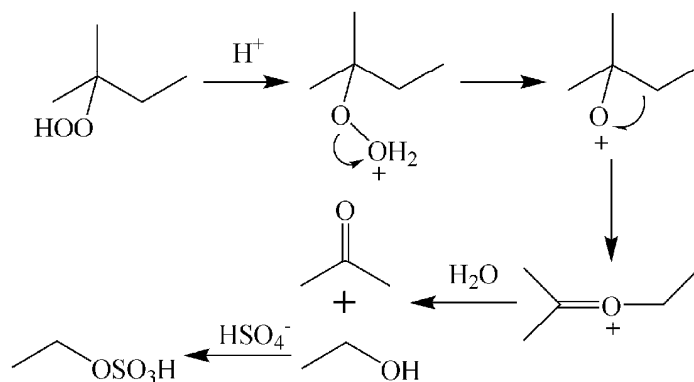
2 **Figure 3.** Typical experimental profiles of TAHP and 3-buten-2-ol. (a) The vacuum
 3 UV mass spectra of TAHP. (b) The profiles of monitoring all ion peaks in real-time
 4 during the uptake of TAHP into 70wt% H_2SO_4 solution. (c) The profiles of monitoring
 5 all ion peaks in real-time during the uptake of 3-buten-2-ol into 70 wt% H_2SO_4
 6 solution. (d) Real-time mass spectrum at the time marked by dash line in (c). (e) The
 7 profiles of monitoring all ion peaks in real-time during the uptake of 3-buten-2-ol into
 8 70 wt% H_2SO_4 -1wt% H_2O_2 mixed solution. (f) Real-time mass spectrum at the time
 9 marked by dash line in (e).

10

11



1

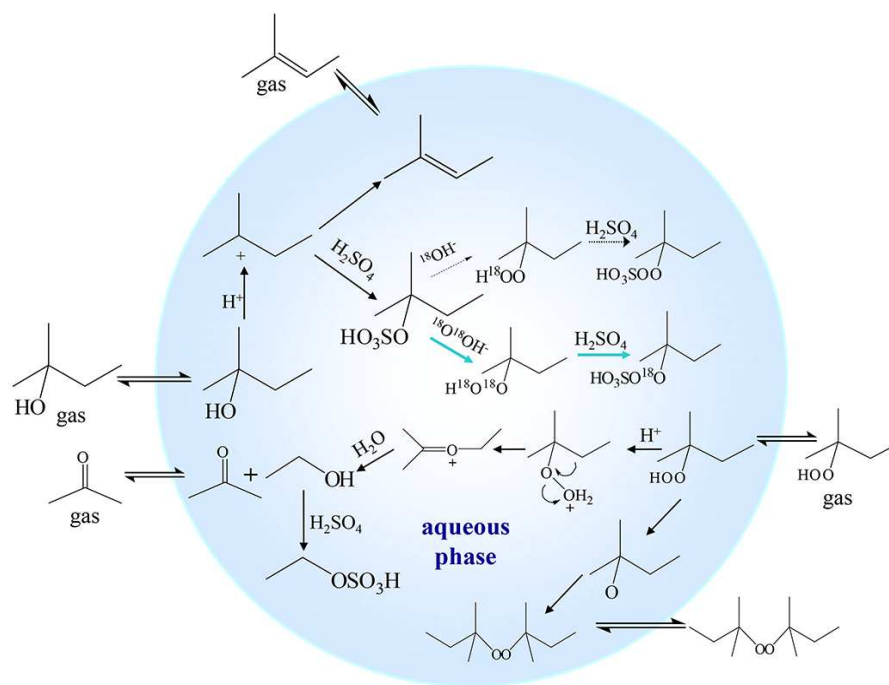
2 **Figure 4.** Proposed chemical mechanism for the formation of TAHP during the3 heterogeneous acid-catalyzed oxidation of 2-methyl-2-butanol with H₂O₂.

4

5 **Figure 5.** Proposed chemical mechanism for the acid-catalyzed rearrangement of

6 TAHP.

Graphical Abstract



We present detailed mechanisms for the formation and degradation of organic hydroperoxide during the acid-catalyzed heterogeneous oxidation of aliphatic alcohols with hydrogen peroxide.